Radiosynthesis and evaluation of ^{18}F-labeled dopamine D_4-receptor ligands

Michael Willmann[a], Johannes Ermert[a]*, Olaf Prante[c], Harald Hübner[d], Peter Gmeiner[d], Bernd Neumaier[a,b]

[a] Forschungszentrum Jülich GmbH, Institut für Neurowissenschaften und Medizin, INM-5, Nuklearchemie, 52425 Jülich, Germany

[b] Uniklinik Köln, Institut für Radiochemie und Experimentelle Molekulare Bildgebung, 50937 Köln, Germany

[c] Friedrich-Alexander University Erlangen-Nürnberg (FAU), Department of Nuclear Medicine, Molecular Imaging and Radiochemistry, Translational Research Center, 91054 Erlangen, Germany

[d] Friedrich-Alexander University Erlangen-Nürnberg (FAU), Department Chemistry and Pharmacy, Medicinal Chemistry, 91058 Erlangen, Germany

* corresponding author: j.ermert@fz-juelich.de

Abbreviated title: ^{18}F-labeled dopamine D_4-receptor ligands

Keywords: ^{18}F-labeling, positron emission tomography, autoradiography, dopamine D_4-receptor, schizophrenia, neurological diseases

A B S T R A C T

Introduction: The dopamine D_4 receptor (D_4R) has attracted considerable attention as potential target for the treatment of a broad range of central nervous system disorders. Although many efforts have been made to improve the performance of putative radioligand candidates, there is still a lack of D_4R selective tracers suitable for *in vivo* PET imaging. Thus, the objective of this work was to develop a D_4-selective PET ligand for clinical applications.

Methods: Four compounds based on previous and new lead structures were prepared and characterized with regard to their D_4R subtype selectivity and predicted lipophilicity. From these, 3-((4-(2-fluorophenyl)piperazin-1-yl)methyl)-1*H*-pyrrolo[2,3-*b*]pyridine **I** and (*S*)-4-(3-fluoro-4-methoxybenzyl)-2-(phenoxymethyl)morpholine **II** were selected for labeling with fluorine-18 and subsequent evaluation by *in vitro* autoradiography to assess their suitability as D_4 radioligand candidates for *in vivo* imaging.

Results: The radiosynthesis of **[^{18}F]I** and **[^{18}F]II** was successfully achieved by copper-mediated radiofluorination with radiochemical yields of 7 % and 66 %, respectively. The radioligand **[^{18}F]II** showed specific binding in areas where D_4 expression is expected, whereas **[^{18}F]I** did not show any uptake in distinct brain regions and exhibited an unacceptable degree of nonspecific binding.

Conclusions: The compounds studied exhibited high D_4R subtype selectivity and log*P* values compatible with high brain uptake, but only ligand **[^{18}F]II** showed low nonspecific binding and is therefore a good candidate for further evaluation.

Advances in Knowledge: The discovery of new lead structures for high-affinity D_4 ligands opens up new possibilities for the development of suitable PET-radioligands.

Implications for patient: PET-imaging of dopamine D_4-receptors could facilitate understanding, diagnosis and treatment of neuropsychiatric and neurodegenerative diseases.

1 Introduction

Dopamine (DA) is an important neurotransmitter involved in cognitive control, reward-related cognition and motor function that produces its effects by interaction with the DA receptors belonging to the G-protein-coupled receptor (GPCR) family. DA D_2 receptor (D_2R) antagonists have a long history as effective antipsychotic drugs, but their clinical application is limited by serious extrapyramidal side effects thought to result from DA receptor blockade in the striatum [1]. The DA D_4 receptor (D_4R), a less abundant member of the D_2-like DA receptor subfamily, has attracted considerable attention as potentially more suitable target for the treatment of central nervous system disorders such as schizophrenia [2], drug abuse [3] and attention deficit hyperactivity disorder [4]. First cloned in 1991, D_4R was identified as a preferential target of the atypical antipsychotic agent clozapine [5] showing a 10 fold higher affinity for the D_4 than for the D_2 receptor [6, 7] (**Fig. 1**), which suggested that selective D_4R antagonism could be responsible for the drugs unique clinical efficacy in otherwise treatment-resistant patients [8]. In addition, early mRNA and immunhistochemical studies indicated that D_4R expression is mostly restricted to extra-striatal (cortical and limbic) brain regions [9, 10], which could explain the very low propensity of clozapine to induce extrapyramidal side effects [11]. However, further studies could not confirm the clinical efficiency of D_4R antagonists in schizophrenia [12, 13] and a number of inconsistent or contradictory findings as well as apparent species differences in receptor distribution have complicated conclusions with regard to the role of D_4R in human health and disease [14, 15]. Imaging techniques like positron emission tomography (PET) could greatly aid in deciphering the physiological and pathophysiological role of D_4R, but their application has been hampered by a number of methodological difficulties. For example, while ligands like L-745,870 (**Fig. 2**) possess subnanomolar affinity and >2,000-fold selectivity for D_4R over D_2R, their aryl piperazine-based structure is common to many GPCR ligands and associated with high off-target affinity (i.e. unspecific binding). The latter could be overcome by rationale drug design based on structure-activity-relationship (SAR) studies, which led to the development of improved ligands with reduced

specific binding to non-D_4 receptors [16, 17]. However, their use for PET imaging studies is further complicated by the low abundance of D_4R in the brain, as even moderate nonspecific binding of radioligand candidates can be sufficient to mask specific binding. While difficult to predict based on SAR studies, nonspecific binding involves partitioning of ligands into phospholipid membranes [18] and often correlates with their lipophilicity/phospholipicity [19-21]. Here, we report our results with four candidate D_4R ligands (**Fig. 3**), which were derived from previous and new lead structures. The potential D_4 selective compounds were synthesized and their dopamine receptor affinities determined. Among these candidates, the two most promising compounds were ^{18}F-labeled and evaluated by means of *in vitro* autoradiography to assess their suitability as D_4 radioligand candidates for *in vivo* imaging.

2 Materials and Methods

2.1 Materials

All chemicals and solvents were purchased by Aldrich (Germany), Fluka (Switzerland), Fluorochem (United Kingdom) and Merck (Germany) and used without any purification. Thin layer chromatography (TLC) was performed on precoated plates of silica gel 60 F254 (Merck, Darmstadt, Germany) and the compounds were detected at 254 nm. All reactions sensitive to moisture were carried out under argon atmosphere in reaction flasks dried overnight at 140 °C prior to use. All reaction mixtures were magnetically stirred. Organic extracts were dried with anhydrous $MgSO_4$ or Na_2SO_4. ^1H, ^{13}C, and ^{19}F NMR spectra were recorded at 400.13, 100.61, and 376.49 MHz, respectively, by means of a Bruker Avance Neo 400 instrument (Bruker Bio Spin GmbH, Rheinstetten, Germany) in 5 % solution at 25 °C. Chemical shifts (δ) are given in parts per million (ppm) relative to trace amounts of the residual solvent signals. High-resolution mass spectrometry (HRMS) analyses were performed using a hybrid linear ion trap FTICR mass spectrometer LTQ-FT (Thermo Fisher Scientific, Bremen, Germany) equipped with a 7 T superconducting magnet by infusion. The mass spectrometer was first tuned and calibrated in the positive mode following the

standard optimization procedure for all voltages and settings. Mass spectra were recorded in full scan from 200 to 1000 Da with a resolution of 100.000 at m/z 400. All data were processed using the Xalibur software version 2.1.

2.2 Syntheses of labeling precursors and reference standards

1*H*-Pyrrolo[2,3-*b*]pyridine-3-carbaldehyde (1): To a solution of 7-azaindole (10.0 g, 84.7 mmol) in acetic acid (20 mL) and H_2O (40 mL) was added HMTA (10.6 g, 75.3 mmol). The reaction mixture was stirred at 120 °C for 6 h. It was cooled with an ice bath, and the resulting precipitate was collected and dried to afford **1** (7.83 g, 71 %) as pale yellow solid. Yield: 7.83 g (71 %); pale yellow solid; *Rf* 0.34 (80 % EtOAc/PE). ^{1}H NMR (400 MHz, DMSO-d6) δ 12.69 (s, 1H), 9.93 (s, 1H), 8.47 (s, 1H), 8.40 (dd, *J* = 7.8, 1.6 Hz, 1H), 8.36 (dd, *J* = 4.7, 1.7 Hz, 1H), 7.27 (dd, *J* = 7.8, 4.7 Hz, 1H).^{13}C NMR (101 MHz, DMSO) δ 185.40, 149.39, 144.83, 138.74, 129.21, 118.42, 116.63, 116.47. MS (ESI): *m*/*z* $[M+H]^+$ calcd for $C_8H_7N_2O^+$: 147.06; found: 147.13. HRMS (ESI): *m*/*z* $[M]^+$ calcd. for $C_8H_5N_2O^+$: 145.03964; found: 145.04075.

Compounds **2** & **3** were synthesized according to a published procedure [22].

.

3-(1-Phenyl-3-propyl-1H-pyrazol-5-yl)propanal (4): To 3-(1-phenyl-3-propyl-1H-pyrazol-5-yl)propan-1-ol (**2**) (1.89 g, 7.74 mmol, 1.0 eq.) in anhydrous DCM (100 mL) at 0 °C (ice bath) was added $NaHCO_3$ (1.30 g; 15.5 mmol, 2.0 eq.) and *Dess-Martin periodinane* (DMP) (3.94 g, 9.29 mmol, 1.2 eq.) under argon. The reaction mixture was stirred for 10 min at 0 °C and then allowed to warm up to ambient temperature. Stirring was continued for 2 h, maintaining the inert atmosphere. Consumption of the starting material was monitored by TLC. The reaction mixture was diluted with a 1:1 mixture of 10 % aq. $Na_2S_2O_3$ and sat. aq. $NaHCO_3$ solution (50 mL) and stirred for 10 min. Et_2O (100 mL) was added and the layers were separated. The organic layer was washed with above 1:1 mixture of 10 % aq. $Na_2S_2O_3$ and sat. aq. $NaHCO_3$ solution (50 mL), dried (Na_2SO_4) and concentrated *in vacuo*. The crude material was purified by flash column chromatography (silica:

EtOAc/PE) to obtain 1.61 g (86 %) of product **4**. *Rf* 0.51 (33 % EtOAc/PE). ^{1}H NMR (200 MHz, $CDCl_3$) δ 9.75 (s, 1H), 7.57 – 7.27 (m, 5H), 6.00 (s, 1H), 3.10 – 2.84 (m, 2H), 2.84 – 2.45 (m, 4H), 1.89 – 1.47 (m, 2H), 0.98 (t, *J* = 7.3 Hz, 3H). ^{13}C NMR (50 MHz, $CDCl_3$) δ 153.78 (s), 142.29 (s), 139.54 (s), 77.79 (s), 77.36 – 76.83 (m), 76.52 (s), 42.67 (s), 30.31 (s), 22.98 (s), 19.01 (s). MS (ESI): *m*/*z* $[M+H]^+$ calcd. for $C_{15}H_{19}N_2O^+$: 243.15; found: 243.20.

***N*-Benzilidene-2-hydroxyethylamine (5):** Benzaldehyde (102.04 mL, 1.00 mol), 2-aminoethanol (60.48 mL, 1.00 mol) and *p*-toluenesulfonic acid (400 mg, 2 mmol) were added to toluene (400 mL). The solution was refluxed for 4 h in a *Dean-Stark* apparatus until 18 mL (1.00 mol) of water were collected in the water trap. The solvent was removed *in vacuo*, dissolved in EtOAc (400 mL) and washed with brine (200 mL) and water (200 mL). After drying ($MgSO_4$) and concentration *in vacuo*, compound **5** (137.00 g, 92 %) was obtained as orange oil. Yield: 137.00 g (92%); orange oil; *Rf* 0.68 (17 % EtOAc/PE). ^{1}H NMR (400 MHz, $CDCl_3$) δ 8.31 (s, 1H), 7.77 – 7.65 (m, 2H), 7.41 (ddd, *J* = 5.4, 4.3, 2.5 Hz, 3H), 3.93 – 3.87 (m, 2H), 3.79 – 3.71 (m, 2H), 3.45 (s, 1H). ^{13}C NMR (101 MHz, $CDCl_3$) δ 163.44, 135.87, 131.03, 128.75, 128.32, 63.41, 62.43. HRMS (ESI): *m*/*z* $[M+Na]^+$ calcd for $C_9H_{11}NONa^+$: 172.07383; found: 172.07335.

2-(Benzylamino)ethanol (6): Compound **5** (20 g, 134 mmol) in 200 mL dry MeOH was chilled in an ice bath and the bottle was flushed with argon. $NaCNBH_3$ (17 g, 270 mmol) was added in portions over the course of 12 h. The complete consumption of starting material was verified by TLC. The reaction mixture was concentrated *in vacuo* and brine (200 mL) was added to the residue, which was then extracted with DCM (3 x 200 mL). The organic layers were washed with water (100 mL), dried and concentrated *in vacuo* to obtain 17.14 g (94 %) of yellow oil of compound **6**, which was purified by acid-base extraction (HCl/NaOH) directly before use. Yield: 17.14 g (94%); yellow oil; *Rf* 0.77 (75 % EtOAc/PE). ^{1}H NMR (400 MHz, Chloroform-*d*) δ 7.28 (tdd, *J* = 14.4, 9.0, 4.8 Hz, 6H), 3.74 (s, 2H), 3.69 – 3.48 (m, 2H), 3.19 (s, 3H), 2.79 – 2.61 (m, 2H). ^{13}C NMR (101 MHz, $CDCl_3$) δ 139.67, 128.58, 128.31, 127.27, 60.82, 53.55, 50.66, 32.22. MS (ESI): *m*/*z* $[M+H]^+$ calcd for $C_9H_{14}NO^+$:

152.11; found: 152.10. HRMS (ESI): *m*/*z* $[M+H]^+$ calcd for $C_9H_{14}NO^+$: 152.10699; found: 152.10703.

(*S*)-(4-Benzylmorpholin-2-yl)methanol (7): To compound **6** (9.64 g, 63.8 mmol) in water (5 mL) and 2-propanol (5 mL) was added (*R*)-epichlorohydrin (5.9 g, 63.8 mmol) and the solution was stirred overnight. A 20 wt-% aqueous solution of Et_4NOH (61 mL, 83.0 mmol) was added over 5 min. After 4 h, the reaction was adjusted to pH 9 with 1 m HCl (10 mL). Water (50 mL) was added and the mixture was extracted with DCM (3 × 500 mL). The extracts were combined and evaporated to an oil, which was purified by flash column chromatography (silica, EtOAc/PE) to afford compound **7**. Yield: 4.66 g (35 %); colorless oil; *Rf* 0.18 (50 % EtOAc/PE). ^{1}H NMR (400 MHz, $CDCl_3$) δ 7.25 (d, *J* = 4.4 Hz, 4H), 7.21 – 7.15 (m, 1H), 3.80 (d, *J* = 1.5 Hz, 1H), 3.64 (dd, *J* = 12.4, 10.0 Hz, 2H), 3.56 – 3.38 (m, 4H), 2.69 – 2.56 (m, 2H), 2.54 – 2.22 (m, 1H), 2.13 (d, *J* = 3.4 Hz, 1H), 2.01 – 1.87 (m, 1H). ^{13}C NMR (101 MHz, $CDCl_3$) δ 129.39, 128.44, 127.44, 76.04, 66.61, 64.23, 63.40, 54.62, 53.07. MS (ESI): *m*/*z* $[M+H]^+$ calcd for $C_{12}H_{18}NO_2^+$: 208.13; found: 208.26. HRMS (ESI): *m*/*z* $[M+H]^+$ calcd for $C_{12}H_{18}NO_2^+$: 208.13321; found: 208.13322.

(*S*)-Morpholin-2-ylmethanol (8): To a stirred mixture of **7** (2.43 g, 12.0 mmol) and 10 % Pd-C (2.43 g) in dry MeOH (80 mL) was added NH_4CO_2H (3.78 g, 60 mmol) in a single portion under nitrogen. This was refluxed for approx. 30 min until TLC showed complete consumption of the starting material. The reaction mixture was filtered through a celite pad, which was then washed with 20 mL $CHCl_3$. Concentration *in vacuo* afforded 1.40 g of product **8**. Yield: 1.40 g (>99 %), pale yellow oil; no UV trace in TLC. ^{1}H NMR (400 MHz, DMSO) δ 4.64 (s, 2H), 3.75 (dd, *J* = 11.4, 2.3 Hz, 1H), 3.58 – 3.21 (m, 4H), 3.17 (s, 1H), 2.90 (d, *J* = 12.1 Hz, 1H), 2.76 (s, 1H), 2.70 (dd, *J* = 11.6, 3.4 Hz, 1H), 2.44 (dd, *J* = 12.2, 10.3 Hz, 1H). ^{13}C NMR (101 MHz, DMSO) δ 76.15, 65.83, 62.47, 47.08, 44.64, 39.52. MS (ESI): *m*/*z* $[M+H]^+$ calcd for $C_5H_{12}NO_2^+$: 118.09; found: 118.15. HRMS (ESI): *m*/*z* $[M+H]^+$ calcd for $C_5H_{12}NO_2^+$: 118.08626; found: 118.08619.

***tert*-Butyl (*S*)-2-(hydroxymethyl)morpholine-4-carboxylate (9): 8** (2.88 g, 24.6 mmol) was added to a stirred solution of guanidine hydrochloride (352 mg, 3.69 mmol) and di-*tert*-butyl dicarbonate

(5.37 g, 24.6 mmol) in EtOH (60 mL) at 40 °C and stirred for 1 h until evolution of CO_2 had ceased. EtOH was evaporated *in vacuo* and the residue was purified by flash column chromatography (silica, EtOAc/PE) to afford the pure product **9**. Yield: 3.07 g (57 %), colorless solid, no UV trace in TLC. ^{1}H NMR (400 MHz, $CDCl_3$) δ 3.82 – 3.60 (m, 1H), 2.86 (dd, *J* = 10.7, 5.8 Hz, 2H), 2.44 (s, 3H), 2.03 (s, 3H), 1.24 (d, *J* = 6.6 Hz, 9H). ^{13}C NMR (101 MHz, $CDCl_3$) δ 143.84, 83.35, 75.15, 62.46, 53.99, 45.63 (s), 29.84, 25.00. MS (ESI): *m*/*z* $[M+H]^+$ calcd for $C_{10}H_{20}NO_4^+$: 218.14; found: 218.23. HRMS (ESI): *m*/*z* $[M+Na]^+$ calcd for $C_{10}H_{19}NNaO_4^+$: 240.12063; found: 240.12074.

***tert*-Butyl (*S*)-2-(phenoxymethyl)morpholine-4-carboxylate (10):** To **9** (500 mg, 2.30 mmol) was added anhydrous THF (1.14 mL), phenol (216 mg, 2.30 mmol) and PPh_3 604 mg, 2.30 mmol). The mixture was sonicated (40 kHz) for several minutes to allow for mixing. More anhydrous THF (1.26 mL) was added slowly until all compounds were dissolved. Under sonification, DIAD (0.454 mL, 2.30 mmol) was added dropwise over a course of 2 min. The mixture was sonicated for further 13 min. Anhydrous $MgCl_2$ (0.44 g, 4.6 mmol) was added and the mixture was refluxed for 2 h, then chilled in an ice bath and filtered to remove the majority of PPh_3O byproduct by complexation. The crude material was purified by flash column chromatography (silica, hexane/EtOAc) and recrystallized from methanol to obtain 259 mg (77 %) of pure product **10**. Yield: 259 mg (77 %), colorless crystals, R*f* 0.60 (33 % EtOAc/PE). ^{1}H NMR (400 MHz, $CDCl_3$) δ 7.26 (s, 2H), 7.07 – 6.77 (m, 3H), 4.08 (ddd, *J* = 15.3, 12.1, 6.2 Hz, 2H), 3.95 (dd, *J* = 9.9, 4.9 Hz, 2H), 3.78 (ddd, *J* = 17.4, 10.1, 7.5 Hz, 1H), 3.65 – 3.54 (m, 1H), 1.47 (s, 9H). ^{13}C NMR (101 MHz, $CDCl_3$) δ 158.67, 154.90, 129.61, 121.30, 114.73, 80.34, 73.98, 70.69, 68.66, 66.76, 29.85, 28.52. MS (ESI): *m*/*z* $[M+H]^+$ calcd for $C_{16}H_{24}NO_4^+$: 294.16; found: 294.22. HRMS (ESI): *m*/*z* $[M+H]^+$ calcd for $C_{16}H_{24}NO_4^+$: 294.16998; found: 294.17003.

(*S*)-(2-Methoxy-5-((2-(phenoxymethyl)morpholino)methyl)phenyl)boronic acid (11): (*S*)-2-(Phenoxymethyl)morpholine (455 mg, 2.35 mmol) and (5-formyl-2-methoxyphenyl)boronic acid (424 mg, 2.35 mmol) in 10 mL MeOH was adjusted to pH 5 with acetic acid. $NaCNBH_3$ (399 mg, 6.36 mmol) was added under argon atmosphere. The mixture was stirred at 60 °C for 24 h. The

reaction mixture was concentrated *in vacuo*. To the residue was added water (20 mL), adjusted to pH 9 with 1 M NaOH and extracted with DCM (3 × 100 mL). The organic layers were dried and concentrated to obtain crude oil, which was purified by flash column chromatography (silica, EtOAc/PE) to provide 423 mg (50 %) of pure product **11**. Yield: 423 mg (50 %); colorless solid. R*f* 0.24 (33 % EtOAc/PE). ^{1}H NMR (400 MHz, $CDCl_3$) δ 7.96 – 7.83 (m, 1H), 7.44 – 7.35 (m, 1H), 7.34 – 7.22 (m, 3H), 6.97 – 6.82 (m, 4H), 4.08 – 3.87 (m, 7H), 3.58 – 3.42 (m, 2H), 2.98 – 2.58 (m, 3H), 2.31 – 2.04 (m, 2H). ^{13}C NMR (101 MHz, $CDCl_3$) δ 163.93, 158.75, 138.33, 133.81, 129.59, 129.39, 128.44, 126.22, 120.93, 114.65, 109.76, 73.90, 69.25, 66.71, 62.70, 55.58, 55.26, 52.85. MS (ESI): *m*/*z* $[M+H]^+$ calcd for $C_{19}H_{25}NO_5^+$: 358.18; found: 358.20. HRMS (ESI): *m*/*z* $[M+H]^+$ calcd for $C_{19}H_{25}BNO_5^+$: 358.18203; found: 358.18202.

3-[4-(2-Fluorophenyl)piperazin-1-yl]-1*H*-pyrrolo-[2,3-*b*]pyridine (I): To **1** (800mg, 5.47mmol) in methanol (14 mL) was added 1-(2-fluorophenyl)piperazine (986 mg, 5.47 mmol). The reaction mixture was adjusted with acetic acid to pH 5 and then reacted with $NaBH_3CN$ (928 mg, 14.77 mmol) at 80 °C for 15 h. After the solvent has been removed *in vacuo*, the residue was diluted with ethyl acetate and neutralized with 10 % NaOH. Product isolation (ethyl acetate) followed by flash column chromatography (silica: EtOAc/PE) afforded compound **I** (611 mg, 36 %) as colorless crystals. Yield: 611 mg (36 %); colorless crystals; R*f* 0.10 (50 %; EtOAc/PE). ^{1}H NMR (400 MHz, DMSO) δ 11.49 (s, 1H), 8.20 (dd, *J* = 4.7, 1.5 Hz, 1H), 8.06 (d, *J* = 6.9 Hz, 1H), 7.39 (s, 1H), 7.17 – 6.86 (m, 5H), 3.70 (s, 2H), 3.33 (s, 2H), 2.99 (s, 4H), 2.57 (s, 3H). ^{13}C NMR (101 MHz, DMSO) δ 156.15, 153.72, 148.73, 142.50, 127.28, 124.79, 122.25, 122.17, 119.77, 119.17, 115.97, 115.76, 115.11, 53.07, 52.41, 50.13. ^{19}F NMR (376 MHz, DMSO) δ -122.79 (s). HRMS (ESI): *m*/*z* $[M+H]^+$ calcd for $C_{18}H_{20}FN_4^+$: 311.16665; found: 311.16662.

(S)-4-(3-Fluoro-4-methoxybenzyl)-2-(phenoxymethyl)morpholine (II): 10 (116 mg, 0.56 mmol) was treated with 1 mL trifluoroacetic acid (TFA) in 3 mL DCM and the mixture was stirred for 1 h at 30 °C. The mixture was then adjusted to pH 9 with 1 m NaOH and extracted with DCM and concentrated *in vacuo* to obtain 104 mg of a crude oil. The unprotected amine (104 mg, 0.54 mmol)

in 2 mL MeOH was added with 3-fluoro-4-methoxybenzaldehyde (83 mg, 054 mmol), the mixture adjusted to pH 5 with acetic acid and $NaBH_3CN$ (92 mg, 2.7 eq.) was added. The mixture was stirred for 16 h at 60 °C. Aqueous workup and extraction with DCM afforded a crude oil, which was purified by flash column chromatography (EtOAc/PE) to obtain compound **11**. Yield: 183 mg (99 %); colorless oil. R*f* 0.44 (33 % EtOAc/PE). ^{1}H NMR (400 MHz, $CDCl_3$) δ 7.33 – 7.19 (m, 4H), 7.16 – 7.06 (m, 2H), 7.04 – 6.82 (m, 10H), 4.07 – 3.84 (m, 14H), 3.73 (td, *J* = 11.3, 2.5 Hz, 2H), 3.45 (s, 4H), 2.85 (d, *J* = 11.1 Hz, 2H), 2.66 (dd, *J* = 11.4, 1.9 Hz, 2H), 2.21 (td, *J* = 11.3, 3.3 Hz, 2H), 2.13 – 2.02 (m, 2H), 1.98 (s, 1H). ^{13}C NMR (101 MHz, $CDCl_3$) δ 158.77, 153.65, 151.21, 146.91, 146.80, 130.89, 129.51, 124.77, 124.73, 121.08, 114.70, 113.19, 113.17, 74.20, 69.23, 66.97, 62.41, 56.40, 55.43, 52.93. ^{19}F NMR (376 MHz, $CDCl_3$) δ -135.43. HRMS (ESI): *m*/*z* $[M+H]^+$ calcd for $C_{19}H_{23}FNO_3^+$: 332.1656; found: 332.1656.

3-((4-(2-Fluorobenzyl)piperazin-1-yl)methyl)-1*H*-pyrrolo[2,3-b]pyridine (III): 1 (225 mg, 1.54 mmol) was dissolved in 5 mL MeOH and 1-(2-fluorobenzyl)piperazine (299 mg, 1.54 mmol) was added thereto. The mixture adjusted to pH 5 with acetic acid and $NaBH_3CN$ (260 mg, 2.7 eq.) was added. The mixture was stirred for 16 h at 60 °C. Aqueous workup and extraction with DCM afforded a crude oil, which was purified by flash column chromatography (silica, EtOAc/PE) to obtain the pure compound **III** as yellow oil. Yield: 250 mg (50 %); yellow oil. R*f* 0.20 (75 % EtOAc/PE). ^{1}H NMR (400 MHz, $CDCl_3$) δ 10.69 (s, 2H), 8.29 (d, *J* = 3.3 Hz, 1H), 8.05 (dd, *J* = 7.9, 1.5 Hz, 1H), 7.33 (t, *J* = 7.5 Hz, 1H), 7.28 (s, 1H), 7.21 (d, *J* = 8.0 Hz, 1H), 7.07 (dd, *J* = 7.3, 5.5 Hz, 2H), 7.04 – 6.95 (m, 1H), 3.73 (s, 2H), 3.59 (s, 2H), 3.28 (s, 2H), 2.55 (s, 8H). ^{13}C NMR (101 MHz, $CDCl_3$) δ 162.77, 160.32, 148.94, 142.62, 131.84, 128.89, 128.29, 124.71, 124.63, 124.49, 123.95, 123.91, 120.85, 115.71, 115.47, 115.25, 110.57, 55.28, 55.26, 53.53, 52.85, 52.77. ^{19}F NMR (376 MHz, $CDCl_3$) δ -117.73. HRMS (ESI): *m*/*z* $[M+H]^+$ calcd for $C_{19}H_{12}FN_4^+$: 325.1823; found: 325.1823.

1-(2-Fluorophenyl)-4-(3-(1-phenyl-3-propyl-1*H*-pyrazol-5-yl)propyl)piperazine (IV): 4 (220 mg, 0.91 mmol) was dissolved in 10 mL of DCM together with 1-(2-fluorophenyl)piperazine (164 mg, 0.91 mmol). To the mixture was added 1.40 g of molecular sieve (4 A). DIPEA (0.16 mL,

0.91 mmol) was slowly added thereto and stirred for 30 min at room temperature. Then, $NaBH(OAc)_3$ (674 mg, 3.18 mmol) was added and stirred at r.t. for 3 d. Water (5 mL) was added and the organic layer was separated and concentrated in vacuo to obtain 404 mg of crude oil, which was purified by flash column chromatography (silica, EtOAc/PE) to obtain 331 mg (90 %) of the pure product **IV** as yellow oil. R*f* 0.20 (33 % EtOAc/PE). ^{1}H NMR (400 MHz, $CDCl_3$) δ 7.56 – 7.30 (m, 5H), 7.11 – 6.82 (m, 4H), 6.05 (s, 1H), 3.24 – 2.93 (m, 4H), 2.81 – 2.45 (m, 8H), 2.46 – 2.27 (m, 2H), 1.89 – 1.58 (m, 4H), 1.00 (t, *J* = 7.4 Hz, 3H). ^{13}C NMR (101 MHz, $CDCl_3$) δ 157.08, 154.63, 153.79, 143.87, 140.30, 140.17, 129.15, 127.62, 125.55, 124.59, 124.55, 122.59, 122.51, 118.99, 116.32, 116.11, 104.46, 77.48, 77.16, 77.16, 76.84, 57.80, 53.32, 50.64, 50.61, 30.51, 26.23, 24.21, 23.10, 14.18. ^{19}F NMR (376 MHz, $CDCl_3$) δ -122.73 (s). HRMS (ESI): *m*/*z* $[M+H]^+$ calcd for $C_{25}H_{32}FN_4^+$: 407.2605; found: 407.2605.

2.3 Receptor binding assay

Radioligand binding studies with the subtypes of the D_2 receptor family were performed as described previously [23]. In brief, competition binding experiments were done using membranes of CHO cells stably expressing the human D_{2L}, D_{2S} [24], D_3 [25] or $D_{4.4}$ [26] receptor. Radioligand displacement assays were run in binding buffer (25 mM HEPES, 5 mM $MgCl_2$, 1 mM EDTA, 0.006% BSA at a pH of 7.4) with [^{3}H]spiperone (molar activity = 68 Ci/mmol, PerkinElmer, Rodgau, Germany). The assays were carried out at a protein concentration of 4 µg/well, B_{max}=1900 fmol/µg, K_D=0.10 nM and a concentration of the radioligand of 0.2 nM for D_{2L}, of 1 µg/well, B_{max}=500 fmol/µg, K_D=0.10 nM and radioligand of 0.2 nM for D_{2S}, of 2 µg/well, B_{max}=3500 fmol/µg, K_D=0.25 nM and radioligand of 0.3 nM for D_3, and of 6 µg/well, B_{max}=1800 fmol/µg, K_D=0.40 nM and radioligand of 0.4 nM for $D_{4.4}$, respectively. Unspecific binding was determined in the presence of 10 µM haloperidol, protein concentration was established by the method of Lowry using bovine serum albumin as standard [27]. Competition binding experiments with GPCRs related to D_2-D_4 were performed in an analogous manner with membranes from HEK293T cells transiently transfected with the corresponding cDNA by using the Mirus TransIT-293 transfection reagent (PeqLab, Erlangen, Germany) or a solution of

polyethylenimine in PBS (PEI, linear 25 kDa, Polysciences, 1 mg/mL) as transfection reagent at a 3:1 PEI to cDNA ratio [28]. Binding to the dopamine receptors D_1 and D_5 was performed with the radioligand [^{3}H]SCH23390 (80 Ci/mmol, Biotrend, Cologne, Germany) at a concentration of 0.30 nM, K_D=0.23 nM, B_{max}=3500 fmol/mg and 2 µg protein/well for D_1, and of 0.50 nM, K_D=0.50 nM, B_{max}=1000 fmol/mg and 14 µg protein/well for D_5, respectively. Affinities to serotonin receptors was measured with [^{3}H]WAY100635 (80 Ci/mmol, Biotrend) at 0.20 nM, K_D=0.10 nM, B_{max}=3000 fmol/mg and 2 µg protein/well for 5-HT_{1A}, and [^{3}H]ketanserin (47 Ci/mmol, Biotrend) at 0.30 nM, K_D=0.35 nM, B_{max}=3400 fmol/mg and 4 µg protein/well for 5-HT_{1A}, respectively. Adrenergic α_{1A} binding was determined applying [^{3}H]prazosin (84 Ci/mmol, Biotrend) at 0.20 nM, K_D=0.095 nM, B_{max}=7500 fmol/mg and 2 µg protein/well.

The resulting competition curves of the receptor binding experiments were analyzed by nonlinear regression using the algorithms in PRISM 6.0 (GraphPad Software, San Diego, CA). The data were initially fit using a sigmoid model to provide an IC_{50} value, representing the concentration corresponding to 50% of maximal inhibition. IC_{50} values were transformed to K_i values according to the equation of *Cheng* and *Prusoff* [29].

2.4 Radiochemistry

All radiosyntheses were carried out using anhydrous *N*,*N*-dimethylacetamide (DMA) (Aldrich). QMA cartridges (Sep-Pak Accell Plus QMA Carbonate Plus Light, 46 mg sorbent per cartridge) were obtained from Waters (Waters GmbH, Eschborn, Germany) and preconditioned with 1 mL H_2O directly before use. [^{18}F]Fluoride was produced by the $^{18}O(p,n)^{18}F$ reaction by bombardment of enriched [^{18}O]water with 16.5 MeV protons using a BC1710 cyclotron (The Japan Steel Works Ltd., Shinagawa, Japan) at the INM-5 (Forschungszentrum Jülich). All radiolabeling experiments were carried out under ambient atmosphere.

Before radiosynthesis, [^{18}F]fluoride was processed as follows. Aqueous [^{18}F]fluoride was loaded onto an anion-exchange resin (QMA cartridge). It should be noted, that aqueous [^{18}F]fluoride was loaded

onto the cartridge from the male side, whereas flushing, washing and $^{18}F^-$ elution were carried out from the female side. If MeOH was used for elution, the resin was flushed with MeOH (2 mL) before use. In order to account for surface-adsorbed [^{18}F]fluoride, reaction vials were completely emptied after the addition of water, and radioactivity in the aqueous solution and remaining radioactivity in the reaction vessel was separately determined and quantified. For radiolabeling, [^{18}F]fluoride was eluted from the QMA cartridge with a solution of Et_4NHCO_3 (1.0 mg) in *n*BuOH (500 µL).

General procedure: The borylated precursor (60 µmol) and $Cu(OTf)_2(py)_4$ (30 µmol) in DMA (600 µL) were added to the dried [^{18}F]fluoride and the reaction mixture was stirred at 110 °C for 10 min, then cooled to room temperature, diluted with water (1 mL) and stirred again for 30 s. Thereafter, RCY was determined by radio-HPLC.

3-((4-(2-[^{18}F]Fluorophenyl)piperazin-1-yl)methyl)-1*H*-pyrrolo[2,3-*b*]pyridine ([^{18}F]I): [^{18}F]Fluoride was eluted from a QMA cartridge with a solution of Et_4NHCO_3 (1.0 mg) in *n*BuOH (500 µL). A solution of tert-butyl 4-(2-(4,4,5,5-tetramethyl-1,3,2-dioxaborolan-2-yl)phenyl)piperazine-1-carboxylate (23 mg, 60 µmol) and $Cu(OTf)_2(py)_4$ (20 mg, 30 µmol) in DMA (600 µL) was added. The reaction mixture was heated at 110 °C for 10 min under air in a capped vial. The solvent was then removed *in vacuo* and 1 mL TFA was added. This was heated for 20 min at 110 °C. TFA was then removed *in vacuo* and **1** (9 mg, 60 µmol) suspended in 2 mL acetonitrile was added. This was heated under reduced pressure and with a steam of argon for azeotropic removal of the ascending water. Then, $NaBH_3CN$ (10 mg) in 1 mL methanol was added and the mixture heated at 80 °C for 5 min. The reaction mixture was quenched with water (4 mL) and passed through a C18 cartridge (500 mg), preconditioned with EtOH (1 mL) and water (10 mL). The cartridge was washed with water (10 mL) and the product was eluted with MeOH (2 mL) and purified by preparative HPLC to afford the desired tracer. HPLC conditions for purification: Synergi 4µ Hydro-RP 150×21.2 mm; eluent: water, 60 % MeCN; flow rate: 6 mL/min; t_R = 5.3 min.

(*S*)-4-(3-[^{18}F]fluoro-4-methoxybenzyl)-2-(phenoxymethyl)morpholine ([^{18}F]II): [^{18}F]Fluoride was eluted from a QMA cartridge with a solution of Et_4NHCO_3 (1.0 mg) in *n*BuOH (500 µL). A

solution of (*S*)-(2-methoxy-5-((2-(phenoxymethyl)morpholino)methyl)phenyl)boronic acid **11** (21 mg, 60 μmol) and $Cu(OTf)_2(py)_4$ (20 mg, 30 μmol) in DMA (600 μL) was added. The reaction mixture was heated at 110 °C for 10 min under air in a capped vial. The reaction mixture was quenched with water (4 mL) and passed through a C18 cartridge (500 mg), preconditioned with EtOH (1 mL) and water (10 mL). The cartridge was washed with water (10 mL) and the product was eluted with MeOH (2 mL) and purified by preparative HPLC to afford [^{18}F]**II.** HPLC conditions for purification: Synergi 4μ Hydro-RP 150×21.2 mm; eluent: water, 60 % MeCN; flow rate: 6 mL/min; t_R = 8.5 min.

2.5 In vitro autoradiography

Wistar rats weighting 250 to 300 g (Charles River Deutschland GmbH) were decapitated, the brains removed and frozen at −80 °C. For autoradiography, they were warmed to −20 °C, cut into 20 μm thick horizontal and sagittal sections (CM 3050 or CM 3500 Polycut, Leica AG Microsystems, Germany), mounted on gelatin-coated object glasses, dried and stored at −80 °C until use.

Autoradiography was performed as described previously [30]. Briefly the frozen brain sections were thawed, dried in air at room temperature and then preincubated for 5 min at ambient temperature in 50 mM Tris HCl (pH 7.4). Sections were then incubated for 70 min in Tris HCl buffer containing a solution of the tracer (2.5 kBq/mL), together or without the “cold” reference compound at a final concentration of 5 μM. Labeling was terminated by rinsing the sections for 1 min in TrisHCl and dipping them in deionized water. The dried sections were placed on a phosphor imaging plate (Fuji) together with a tritium standard (Amersham Bioscience). After exposure for 75 minutes, a laser phosphor imager (BAS 5000, Fuji) controlled with software from the vendor (Version 3.14, Raytest, Germany) was used for image acquisition.

2.6 HPLC Analysis

Before the determination of radiochemical yield (RCY), reaction mixtures were diluted with 50% MeOH to dissolve any [^{18}F]fluoride adsorbed onto the reaction vessel walls. HPLC analyses were

carried out on a Dionex Ultimate® 3000 HPLC system and a DAD UV-detector coupled in series with a Berthold NaI detector. A Chromolith® SpeedROD RP-18e column (Merck, Darmstadt Germany), 50×4.6 mm was used. UV and radioactivity detectors were connected in series, giving a time delay of 0.1–0.9 min depending on the flow rate. ^{18}F-Labeled compounds were identified by co-injection of the unlabeled reference compounds using HPLC. The completeness of the radioactivity elution was checked by analyzing the same sample amount choosing a column bypass. Column: Chromolith SpeedROD®, 50×4.6 mm (Merck Millipore); gradient: 0–2 min: 5 % MeCN, 2–2.5 min: 5→20 % MeCN, 2.5–6 min: 20 % MeCN, 6–7 min: 20→70 % MeCN, 7–9 min: 70 % MeCN, flow rate: 3.0 mL/min.

2.7 Determination of carrier content

The amount of unlabeled carrier was determined from the peak area in UV–HPLC chromatograms using an UV absorbance/concentration calibration curve ([^{18}F]**I**: λ = 223 nm; [^{18}F]**II**: λ = 256 nm). The solutions of radiolabeled products obtained after HPLC purification were allowed to stand at ambient temperature for at least 24 h, concentrated under reduced pressure, and the residues were re-dissolved in the appropriate HPLC eluents (500 μL). The resulting solutions were completely injected into the HPLC system. The peak area was determined, and the amount of carrier was calculated according to the calibration curve.

2.8 Estimation of lipophilicity

The software program ChemDraw 16.0 (PerkinElmer) using Crippen's fragmentation method [31] and the online tools ALOGPS 2.1 [32] and Chemicalize [33] were used for the estimation of Log*P* values.

3 Results and discussion

*3.1 Synthesis of reference compounds **I-IV** and labeling precursor **12***

Based on azaindoles like L-745.870 [34, 35], FAUC 113/213 [36-38], ABT-124 [39, 40] or PIP3EA [41] as D_4R selective lead structures, compounds **I** and **III** were prepared by reductive amination of

1*H*-Pyrrolo[2,3-*b*]pyridine-3-carbaldehyde **1** and 1-(2-fluorophenyl)piperazine (2-FPP) (for **I**, see scheme 1) or 1-(2-fluorobenzyl)piperazine (for **III**, see scheme 2) using $NaBH_3CN$ as reductant.

To obtain 1*H*-pyrrolo[2,3-*b*]pyridine-3-carbaldehyde **1**, a formylation of 7-azaindol was carried out using either the *Vilsmeier-Haack reaction* [42] or the *Duff reaction* [43], with the Duff reaction performing better in terms of yield (71%) and ease of work-up.

Reference compound **IV** was chosen based on D_4R selective piperazinyl-propyl-pyrazole derivatives as alternative lead structures and synthesized according to a known procedure modified only by the use of the less toxic oxidant *Dess-Martin periodinane* (DMP) in the oxidation step (Scheme 3) [22].

The synthesis of the chiral alkoxy morpholines **II** and **12** was achieved according to a procedure from HENEGAR [44] (Scheme 4), starting with the condensation of benzaldehyde and 2-aminoethanol under *Dean-Stark* conditions, yielding the benzyl-protected ethanolamine **6** (94 %) after reduction of the aldimine **5** by $NaBH_4$ (92 %). Chirality was introduced by the reaction of **6** with enantiomerically pure (*R*)-epichlorohydrin, yielding an intermediate chlorohydrin (Scheme 4). Without isolation of the intermediate, the cyclization reaction forming the epoxide was initiated by addition of Et_4NOH. Under inversion of the configuration (*Walden inversion*), the epoxide underwent further cyclization to form the morpholine oxide **7** in a yield of 35 %. Subsequent *Mitsunobu reaction* [45] with the phenol of either the *N*-benzyl or the *N*-Boc protected morpholine proceeded under sonification (40 kHz) in 15 minutes with comparable yields, but reductive cleavage (HCO_2NH_4, 10 % Pd-C) of the benzyl group, which was used as a chromophore for reaction monitoring, gave significantly better yields (77 %) when it was performed prior to *Mitsunobu* coupling. Since the *Mitsunobu* reaction failed with the unprotected morpholine, it was again protected with the easily removable *N*-Boc group in a yield of 57 %. Reductive amination ($NaBH_3CN$) with either 3-fluoro-4-methoxybenzaldehyde or (5-formyl-2-methoxyphenyl)boronic acid yielded the reference compound **II** (99 %) or the radiolabeling precursor **12** (50 %) respectively. Enantiomeric purity (>99 %) was conserved for both compounds throughout the synthesis and verified by chiral HPLC.

3.2 Receptor binding studies

The target compounds **I-IV** were subjected tabto *in vitro* receptor binding assays to test their ability to displace [^{3}H]SCH 23990 from the cloned human D_1-like DA receptors D_1R and D_5R, or [^{3}H]spiperone from the cloned human D_2-like DA receptors D_2Rlong, D_2Rshort, D_3R and the most common D_4R polymorphism $D_{4.4}R$, which were stably expressed in Chinese hamster ovary (CHO) cells. In addition, binding to the cloned human serotonin receptors 5-$HT_{1A}R$ and 5-$HT_{2A}R$ as well as the cloned human alpha adrenergic receptor α_{1A} transiently transfected in human embryonic kidney (HEK293T) cells were examined by displacement experiments with the selective radioligands [^{3}H]WAY600135, [^{3}H]ketanserin and [^{3}H]prazosin respectively. The results of these experiments are summarized in **Tab. 1**. All compounds exhibited high affinity for the D_4 receptor subtype with K_i values ranging from 4.1 to 18 nM (**Tab. 1**) and, except for compound **IV**, reduced affinity for all other receptors tested (**Tab. 2**). Based on its very high affinity for the human α_{1A} receptor (K_i=1.2 nM, **Tab. 1 & 2**) combined with a high predicted lipophilicity (see below), compound **IV** was excluded from further studies. In comparison with reported D_4-subtype selective ligands, such as FAUC 213 with a D_4-over-D_3 selectivity of 2400-fold [37], compound **III** showed very similar D_4 subtype selectivity (2000-fold, **Tab. 2**), but its D_4 affinity (K_i=18 nM, **Tab. 1**) was almost ten-fold lower than that of FAUC 213 (2 nM). However, the outstanding subtype selectivity and very low affinity for 5-HT receptors suggested that this compound might still be worthwhile for radiolabeling and future *in vivo* studies. The highest affinity for the D_4 receptor was found for the 2-fluorophenylpiperazinyl 7-azaindole (**I**) (K_i=4.1 nM), which exhibited moderate to good selectivity over 5-HT (140 to 3400-fold) and D_2 (230 to 340-fold) receptors (**Tab. 2**). The morpholine derivative (**II**) showed a less variable D_4-over-5-HT selectivity (570 to 610-fold) but only low D_4-subtype selectivity (35 to 36-fold) (**Tab. 2**). Thus, taken together, ligand **I** and **II** both revealed adequate D_4 affinity combined with variable affinities to 5-HT (**I** > **II**) and non-D_4 DA (**I** < **II**) receptors.

3.3 Lipophilicity

A number of previous studies indicate that blood-brain-barrier (BBB) penetration and nonspecific binding are often correlated with the lipophilicity of a ligand. To obtain a rough measure of this

physiochemical property, various tools were used to calculate log*P* and log$D_{7.4}$ values for compounds **I**-**IV**. As illustrated in **Tab. 3**, the different algorithms showed similar results, with values determined to be between 2 and 3 for compounds **I**-**III**, a range considered optimal for ligands to penetrate the blood-brain-barrier without excessive nonspecific binding. In contrast and as already noted above, values between 5 and 6 were obtained for compound **IV**, suggesting that nonspecific binding of this ligand could be high. Therefore, **IV** was not selected for radiosynthesis and excluded from further evaluation.

3.4 Radiosynthesis

Due to their promising D_4 selectivities, compounds **I** & **II** were selected for radiolabeling and subsequent *in vitro* autoradiographic studies. The synthesis of radiotracer [^{18}F]**I** was performed by a three-step one-pot reaction without the need for isolation of any intermediates (Scheme 5). Attempts for late stage radiofluorination were not successful since the corresponding *ortho*-borylated precursor for [^{18}F]**I** was challenging to synthesize and degraded upon purification by column chromatography.

The [^{18}F]fluoride used for radiofluorination was trapped on a QMA cartridge and eluted with tetraethylammonium bicarbonate (TEAHC) in *n*-butanol with an elution efficacy of 90 ± 5 %.

A Cu(II)-mediated radiofluorination protocol as described by ZISCHLER et al. [46], with commercially available *tert*-butyl 4-(2-(4,4,5,5-tetramethyl-1,3,2-dioxaborolan-2-yl)phenyl)piperazine-1-carboxylate as the precursor was performed at 110 °C for 10 min, which led to [^{18}F]**13** in 60-80 % radiochemical yield (RCY). Deprotection was achieved with excess trifluoroacetic acid (TFA) at 110 °C for 20 min. Under less harsh conditions, deprotection did not proceed quantitatively. Subsequently, the D_4R-radioligand [^{18}F]**I** was obtained by reductive amination with azaindole 3-carbaldehyde **1**, using an excess of $NaBH_3CN$ as reductant, for 5 min at 80 °C. The crude solution was passed through a C18 cartridge to trap the product, washed with water and eluted with methanol. [^{18}F]**I** was then isolated by semi-preparative HPLC with a total RCY of 7 %.

Precursor **11** (Scheme 6) was used for aromatic nucleophilic ^{18}F-substitution with the same Cu(II)-mediated radiofluorination protocol by ZISCHLER et al. as used above [46]. [^{18}F]Fluoride was trapped on a QMA cartridge and eluted with tetraethylammonium bicarbonate (TEAHC) into a solution of **11** and [Cu(OTf)$_2$(py)$_4$] in *N*,*N*-dimethylacetamide (DMA) and reacted at 110 °C for 10 min to obtain [^{18}F]**II**. The crude solution was passed through a C18 cartridge to trap the product, washed with water and eluted with methanol. Finally, the radiotracer [^{18}F]**II** was (partially) isolated by semi-preparative HPLC with a RCY of 66% (n=5).

3.5. Autoradiography

The main reason for failure of D$_4$R selective radioligand candidates in *in vivo* experiments is a high ratio of nonspecific to specific binding. Here, we used *in vitro* autoradiography in competition with the non-labeled reference compounds to determine nonspecific binding of the radiolabeled compounds **[^{18}F]I** and **[^{18}F]II.** To this end, rat brain slices were incubated either with the labeled compounds alone (total binding) or with the labeled compounds and an excess of the corresponding non-labeled reference compound (non-specific binding).

In three independent experiments with molar activities of up to 90 GBq/µmol, the D$_4$ receptor ligand **[^{18}F]I** did not show any uptake in distinct brain regions and exhibited an unacceptably high degree of non-specific binding that could not be displaced by the non-radioactive reference compound (**Fig. 4**). Thus, **[^{18}F]I** is presumably unsuitable for *in vivo* PET imaging applications and was therefore excluded from further studies.

For comparison, **Fig. 5** shows horizontal and sagittal rat brain slices incubated with the chiral radioligand **[^{18}F]II** at a molar activity of 80 GBq/µmol (starting activity: 2450 MBq). Due to the relatively low molar activity that was achieved by the manual radiosynthesis, the signal-to-noise ratio of the autoradiography images could most likely be further improved by the use of an automated synthesis module.

In any case, **[^{18}F]II** appeared to show specific binding throughout the brain, with no uptake in the striatum but distinct high accumulation in the colliculi and medial nuclei of the cerebellum (**Fig. 5**), which is in line with previous results obtained using *in vitro* autoradiography with [^{18}F]FPPB by KÜGLER et al. [21]. On the other hand, little binding was observed in prefrontal cortex (PFC) and hippocampus (HC), even though mRNA [9], immunhistochemical [15, 47, 48] and autoradiographic [21, 49, 50] findings indicate predominant expression of D_4R in these regions of the rat brain. Interestingly, lack of binding in PFC and HC was also observed in previous *in vitro* autoradiography experiments with [^{18}F]FPPB, while *ex vivo* autoradiography with the same radioligand revealed clear binding in these regions [21]. With this in mind, our findings encourage further evaluation of **[^{18}F]II** brain uptake and distribution in preclinical animal models by PET.

4. Conclusion

In summary, four compounds that appeared suitable for the development of a D_4-selective radioligand for PET imaging were first examined for their D_4R subtype selectivity. Based on the properties found, two of the compounds were ^{18}F-labeled and examined by *in vitro* autoradiography. Of these, only ligand (*S*)-4-(3-[^{18}F]fluoro-4-methoxybenzyl)-2-(phenoxymethyl)morpholine **[^{18}F]II** showed low non-specific binding and accumulation in distinct, extra-striatal brain regions. Further work is in progress to study the brain uptake and metabolism of **[^{18}F]II** in preclinical animal models.

5. Acknowledgement

The authors would like to thank Annette Schulze, Dr. Dirk Bier and Dr. Marcus Holschbach (all INM-5), and Dr. Sabine Willbold (Zentralinstitut für Engineering, Elektronik und Analytik, ZEA-3), all Forschungszentrum Jülich, for recording the spectroscopic data and conducting the biological studies.

References

1. Reynolds GP. Developments in the drug treatment of schizophrenia. Trends in Pharmacological Sciences 1992;13:116-21.
2. Sanyal S, Van Tol HHM. Review the role of dopamine D_4 receptors in schizophrenia and antipsychotic action. J Psychiatr Res 1997;31:219-32.
3. Di Ciano P, Grandy DK, Le Foll B. Chapter Eight - Dopamine D_4 Receptors in Psychostimulant Addiction In: Dwoskin L P Advances in Pharmacology Academic Press 2014, p 301-21.
4. Sunohara GA, Roberts W, Malone M, Schachar RJ, Tannock R, Basile VS, Wigal T, Wigal SB, Schuck S, Moriarty J, Swanson JM, Kennedy JL, Barr CL. Linkage of the Dopamine D_4 Receptor Gene and Attention-Deficit/Hyperactivity Disorder. J Am Acad Child Adolesc Psychiatry 2000;39:1537-42.
5. Van Tol HHM, Bunzow JR, Guan H-C, Sunahara RK, Seeman P, Niznik HB, Civelli O. Cloning of the gene for a human dopamine D_4 receptor with high affinity for the antipsychotic clozapine. Nature 1991;350:610-4.
6. Strange PG, Neve K. Dopamine Receptors. Tocris Scientific Review Series 2013:1-11.
7. Roth B, Lopez E, *PDSP Ki Database. Psychoactive Drug Screening Program (PDSP)*. (accessed on 15.07.2019); Available online: https://pdsp.unc.edu/databases/kidb.php.
8. Kane J, Honigfeld G, Singer J, Meltzer H. Clozapine for the Treatment-Resistant Schizophrenic: A Double-blind Comparison With Chlorpromazine. Arch Gen Psychiatry 1988;45:789-96.
9. O'Malley KL, Harmon S, Tang L, Todd RD. The rat dopamine D_4 receptor: sequence, gene structure, and demonstration of expression in the cardiovascular system. New Biol 1992;4:137-46.

10. Meador-Woodruff JH, Damask SP, Wang J, Haroutunian V, Davis KL, Watson SJ. Dopamine Receptor mRNA Expression in Human Striatum and Neocortex. Neuropsychopharmacology 1996;15:17-29.

11. Ackenheil vM, Braeu H. Antipsychotische Wirksamkeit im Verhältnis zum Plasmaspiegel von Clozapin. Arzneimittelforschung. Arzneimittelforschung 1976;26:1156–8.

12. Kramer MS, Last B, Getson A, Reines SA. The Effects of a Selective D_4 Dopamine Receptor Antagonist (L-745,870) in Acutely Psychotic Inpatients With Schizophrenia. Arch Gen Psychiatry 1997;54:567-72.

13. Truffinet P, Tamminga CA, Fabre LF, Meltzer HY, Riviï¿½re M-E, Papillon-Downey C. Placebo-Controlled Study of the D_4/5-HT_{2A} Antagonist Fananserin in the Treatment of Schizophrenia. Am J Psychiatry 1999;156:419-25.

14. Helmeste DM, Tang SW. Dopamine D_4 Receptors. Jpn J Pharmacol 2000;82:1-14.

15. Khan ZU, Gutiérrez A, Martín R, Peñafiel A, Rivera A, De La Calle A. Differential regional and cellular distribution of dopamine D_2-like receptors: An immunocytochemical study of subtype-specific antibodies in rat and human brain. J Comp Neurol 1998;402:353-71.

16. Lanig H, Utz W, Gmeiner P. Comparative Molecular Field Analysis of Dopamine D_4 Receptor Antagonists Including 3-[4-(4-Chlorophenyl)piperazin-1-ylmethyl]pyrazolo[1,5-*a*]pyridine (FAUC 113), 3-[4-(4-Chlorophenyl)piperazin-1-ylmethyl]-1H-pyrrolo[2,3-*b*]pyridine (L-745,870), and Clozapine. J Med Chem 2001;44:1151-7.

17. Kortagere S, Gmeiner P, Weinstein H, Schetz JA. Certain 1,4-disubstituted aromatic piperidines and piperazines with extreme selectivity for the dopamine D_4 receptor interact with a common receptor microdomain. Mol Pharmacol 2004.

18. Nagar S, Korzekwa K. Nonspecific Protein Binding Versus Membrane Partitioning - It Is Not Just Semantics. Drug Metab Dispos 2012;40:1649-52.

19. Wang Y, Mathis CA, Huang G-F, Debnath ML, Holt DP, Shao L, Klunk WE. Effects of lipophilicity on the affinity and nonspecific binding of iodinated benzothiazole derivatives. J Mol Neurosci 2003;20:255-60.

20. Sebai S, Baciu M, Ces O, Clarke J, Cunningham V, Gunn R, Law R, Mulet X, Parker C, Plisson C, Templer R, Gee A. To lipophilicity and beyond—towards a deeper understanding of radioligand non-specific binding. NeuroImage 2006;31:T56.

21. Kügler F, Sihver W, Ermert J, Hübner H, Gmeiner P, Prante O, Coenen HH. Evaluation of ^{18}F-labeled benzodioxine piperazine-based dopamine D_4 receptor ligands: Lipophilicity as a determinate of nonspecific binding. J Med Chem 2011;54:8343-52.

22. Kong JY, Park WK, Cho H, Jeong D, Choi G, Koh HY, Kim SH, Pae AN, Cho YS, Cha JH (2007) Piperazinyl-propyl-pyrazole derivatives as dopamine D_4 receptor antagonists, and pharmaceutical compositions containing the same. Patent WO2008108517A2.

23. Hübner H, Haubmann C, Utz W, Gmeiner P. Conjugated Enynes as Nonaromatic Catechol Bioisosteres: Synthesis, Binding Experiments, and Computational Studies of Novel Dopamine Receptor Agonists Recognizing Preferentially the D_3 Subtype. J Med Chem 2000;43:756-62.

24. Hayes G, Biden TJ, Selbie LA, Shine J. Structural subtypes of the dopamine D_2 receptor are functionally distinct: expression of the cloned D_{2A} and D_{2B} subtypes in a heterologous cell line. Mol Endocrinol 1992;6:920-6.

25. Sokoloff P, Giros B, Martres MP, Bouthenet ML, Schwartz JC. Molecular cloning and characterization of a novel dopamine receptor (D_3) as a target for neuroleptics. Nature 1990;347:146-51.

26. Asghari V, Sanyal S, Buchwaldt S, Paterson A, Jovanovic V, Van Tol HHM. Modulation of Intracellular Cyclic AMP Levels by Different Human Dopamine D_4 Receptor Variants. J Neurochem 1995;65:1157-65.

27. Lowry OH, Rosebrough NJ, Farr AL, Randall RJ. Protein measurement with the Folin phenol reagent. J Biol Chem 1951;193:265-75.

28. Möller D, Banerjee A, Uzuneser TC, Skultety M, Huth T, Plouffe B, Hübner H, Alzheimer C, Friedland K, Müller CP, Bouvier M, Gmeiner P. Discovery of G Protein-Biased Dopaminergics with a Pyrazolo[1,5-*a*]pyridine Substructure. J Med Chem 2017;60:2908-29.

29. Cheng Y, Prusoff WH. Relationship Between the Inhibition Constant (K_I) and the Concentration of Inhibitor Which Causes 50 Per Cent Inhibition (I_{50}) of an Enzymatic Reaction Biochem Pharmacol 1973;22:3099-108.

30. Sihver W, Bier D, Holschbach MH, Schulze A, Wutz W, Olsson RA, Coenen HH. Binding of tritiated and radioiodinated ZM241,385 to brain A_{2A} adenosine receptors. Nucl Med Biol 2004;31:173-7.

31. Ghose AK, Crippen GM. Atomic physicochemical parameters for three-dimensional-structure-directed quantitative structure-activity relationships. 2. Modeling dispersive and hydrophobic interactions. J Chem Inf Comput Sci 1987;27:21-35.

32. Tetko IV, Gasteiger J, Todeschini R, Mauri A, Livingstone D, Ertl P, Palyulin VA, Radchenko EV, Zefirov NS, Makarenko AS, Tanchuk VY, Prokopenko VV. Virtual Computational Chemistry Laboratory – Design and Description. J Comput Aided Mol Des 2005;19:453-63.

33. *Chemicalize was used for prediction of LogP & LogD values*. (accessed on 26. July 2020); Available online: http://www.chemaxon.com.

34. Kulagowski JJ, Broughton HB, Curtis NR, Mawer IM, Ridgill MP, Baker R, Emms F, Freedman SB, Marwood R, Patel S, Patel S, Ragan CI, Leeson PD. 3-[[4-(4-Chlorophenyl)piperazin-1-yl]methyl]-1*H*-pyrrolo[2,3-*b*]pyridine: An Antagonist with High Affinity and Selectivity for the Human Dopamine D_4 Receptor. J Med Chem 1996;39:1941-2.

35. Gazi L, Bobirnac I, Danzeisen M, Schüpbach E, Langenegger D, Sommer B, Hoyer D, Tricklebank M, Schoeffter P. Receptor density as a factor governing the efficacy of the dopamine D_4 receptor ligands, L-745,870 and U-101958 at human recombinant $D_{4.4}$ receptors expressed in CHO cells. Br J Pharmacol 1999;128:613-20.

36. Löber S, Hübner H, Gmeiner P. Azaindole derivatives with high affinity for the dopamine D_4 receptor: Synthesis, ligand binding studies and comparison of molecular electrostatic potential maps. Bioorg Med Chem Lett 1999;9:97-102.

37. Löber S, Hübner H, Utz W, Gmeiner P. Rationally Based Efficacy Tuning of Selective Dopamine D_4 Receptor Ligands Leading to the Complete Antagonist 2-[4-(4-Chlorophenyl)piperazin-1- ylmethyl]pyrazolo[1,5-*a*]pyridine (FAUC 213). J Med Chem 2001;44:2691-4.

38. Boeckler F, Russig H, Zhang W, Löber S, Schetz J, Hübner H, Ferger B, Gmeiner P, Feldon J. FAUC 213, a highly selective dopamine D_4 receptor full antagonist, exhibits atypical antipsychotic properties in behavioural and neurochemical models of schizophrenia. Psychopharmacology 2004;175:7-17.

39. Cowart M, Latshaw SP, Bhatia P, Daanen JF, Rohde J, Nelson SL, Patel M, Kolasa T, Nakane M, Uchic ME, Miller LN, Terranova MA, Chang R, Donnelly-Roberts DL, Namovic MT, Hollingsworth PR, Martino BR, Lynch JJ, Sullivan JP, Hsieh GC, Moreland RB, Brioni JD, Stewart AO. Discovery of 2-(4-Pyridin-2-ylpiperazin-1-ylmethyl)-1*H*-benzimidazole (ABT-724), a Dopaminergic Agent with a Novel Mode of Action for the Potential Treatment of Erectile Dysfunction. J Med Chem 2004;47:3853-64.

40. Brioni JD, Moreland RB, Cowart M, Hsieh GC, Stewart AO, Hedlund P, Donnelly-Roberts DL, Nakane M, Lynch JJ, Kolasa T, Polakowski JS, Osinski MA, Marsh K, Andersson K-E, Sullivan JP. Activation of dopamine D_4 receptors by ABT-724 induces penile erection in rats. Proc Natl Acad Sci USA 2004;101:6758-63.

41. Enguehard-Gueiffier C, Hübner H, El Hakmaoui A, Allouchi H, Gmeiner P, Argiolas A, Melis MR, Gueiffier A. 2-[(4-Phenylpiperazin-1-yl)methyl]imidazo(di)azines as Selective D_4-Ligands. Induction of Penile Erection by 2-[4-(2-Methoxyphenyl)piperazin-1-ylmethyl]imidazo[1,2-*a*]pyridine (PIP3EA), a Potent and Selective D_4 Partial Agonist. J Med Chem 2006;49:3938-47.

42. Yadav RR, Battini N, Mudududdla R, Bharate JB, Muparappu N, Bharate SB, Vishwakarma RA. Deformylation of indole and azaindole-3-carboxaldehydes using anthranilamide and solid acid heterogeneous catalyst via quinazolinone intermediate. Tetrahedron Lett 2012;53:2222-5.

43. Jia H, Dai G, Weng J, Zhang Z, Wang Q, Zhou F, Jiao L, Cui Y, Ren Y, Fan S, Zhou J, Qing W, Gu Y, Wang J, Sai Y, Su W. Discovery of (S)-1-(1-(Imidazo[1,2-*a*]pyridin-6-yl)ethyl)-6-(1-methyl-1*H*-pyrazol-4-yl)-1*H*-[1,2,3]triazolo[4,5-*b*]pyrazine (Volitinib) as a Highly Potent and Selective Mesenchymal–Epithelial Transition Factor (c-Met) Inhibitor in Clinical Development for Treatment of Cancer. J Med Chem 2014;57:7577-89.

44. Henegar KE. Concise Synthesis of (S)-N-BOC-2-Hydroxymethylmorpholine and (S)-N-BOC-Morpholine-2-carboxylic Acid. J Org Chem 2008;73:3662-5.

45. Lepore SD, He Y. Use of Sonication for the Coupling of Sterically Hindered Substrates in the Phenolic Mitsunobu Reaction. J Org Chem 2003;68:8261-3.

46. Zischler J, Kolks N, Modemann D, Neumaier B, Zlatopolskiy BD. Alcohol-Enhanced Cu-Mediated Radiofluorination. Chem Eur J 2017;23:3251-6.

47. Defagot MC, Malchiodi EL, Villar MJ, Antonelli MC. Distribution of D_4 dopamine receptor in rat brain with sequence-specific antibodies. Mol Brain Res 1997;45:1-12.

48. Ariano MA, Wang J, Noblett KL, Larson ER, Sibley DR. Cellular distribution of the rat D_4 dopamine receptor protein in the CNS using anti-receptor antisera. Brain Res 1997;752:26-34.

49. Prante O, Tietze R, Hocke C, Löber S, Hübner H, Kuwert T, Gmeiner P. Synthesis, Radiofluorination, and In Vitro Evaluation of Pyrazolo[1,5-*a*]pyridine-Based Dopamine D_4 Receptor Ligands: Discovery of an Inverse Agonist Radioligand for PET. J Med Chem 2008;51:1800-10.

50. Primus RJ, Thurkauf A, Xu J, Yevich E, McInerney S, Shaw K, Tallman JF, Gallagher DW. II. Localization and characterization of dopamine D_4 binding sites in rat and human brain by use of the novel, D_4 receptor-selective ligand [^{3}H]NGD 94-1. J Pharmacol Exp Ther 1997;282:1020-7.

Figures Capture:

Figure 1. The first atypical antipsychotic clozapine in comparison with typical antipsychotics.

Figure 2. D_4 selective receptor ligands **ABT-724** and **L-745,870** with binding affinities and calculated Log*P* values (ChemDraw 16).

Figure 3. Compounds selected for binding studies

Figure 4. *In vitro* autoradiography of horizontal rat brain slices with 2.31 kBq/mL [^{18}F]I alone (Total binding) or after blocking with 5 µM non-labeled I (Non-specific binding). i) Total binding profile. ii) Competition with non-radioactive [^{19}F]I, displaying non-specific binding.

Figure 5. *In vitro* autoradiography of horizontal (top) and sagittal (bottom) rat brain slices with 2.31 kBq/mL [^{18}F]II alone (Total binding) or after blocking with 5 µM non-labeled II (Nonspecific binding). cbl: cerebellum, co: colliculi, c: cortex).

Scheme 1. Synthesis of reference compound I a) Hexamethylenetetramine (HMTA, 120 °C, 6 h). b) 1-(2-fluorophenyl)piperazine, $NaBH_3CN$, pH 5 (AcOH), 80 °C, 15 h.

Scheme 2. Synthesis of reference compound **III** a) 1-(2-fluorobenzyl)piperazine, $NaBH_3CN$, pH 5 (AcOH), 80 °C, 15 h.

Scheme 3. Synthesis of reference compound **IV** a) NaOMe, benzene, 30-50 °C. b) TEA 3 eq., MeOH, r.t., 4 h. c) DMP, DCM, r.t., 12 h. d) $NaBH_3CN$, MeOH, 80 °C, 12 h.

Scheme 4. Synthesis of labeling precursor **22** and reference compound **II** a) 2-aminoethanol, toluene b) $NaBH_3CN$, r.t., 12 h. c) (*R*)-epichlorhydrine d&e) 20 wt-% aq. Et_4NOH, 2-PrOH/H2O (1:1) f)

10 % Pd-C, NH_4CO_2H, MeOH g) guanidine*HCl, di-*tert*-butyl dicarbonate, EtOH h) phenol, PPh_3, diisopropyl azodicarboxylate (DIAD), THF, 40 kHz, 15 min i) HCl, $NaBH_3CN$, MeOH, 60 °C, 12 h.

Scheme 5. Synthesis of compound [^{18}F]**I** a) Elution of ^{18}F- with Et_4NHCO_3 in *n*BuOH; $[Cu(OTf)_2(py)_4]$, DMA, 110 °C, 10 min. b) TFA, 110 °C, 20 min. c) **3**, $NaBH_3CN$, 80 °C, 5 min. (RCY determined by radio-HPLC).

Scheme 6. Synthesis of compound **[^{18}F]II** a) Elution of $^{18}F^-$ with Et_4NHCO_3 in *n*BuOH; $[Cu(OTf)_2(py)_4]$, DMA, 110 °C, 10 min.

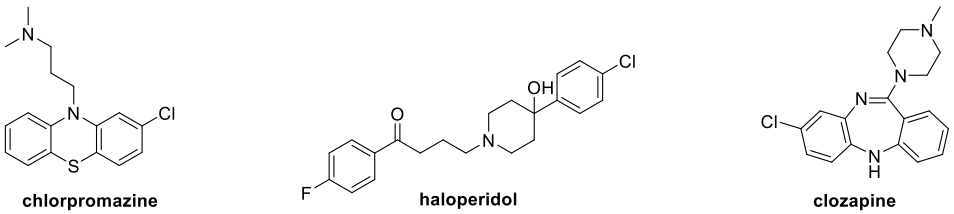

chlorpromazine	haloperidol	clozapine
$K_i(D_1)$ 90 nM	$K_i(D_1)$ 80 nM	$K_i(D_1)$ 170 nM
$K_i(D_2)$ 3 nM	**$K_i(D_2)$ 1.2 nM**	$K_i(D_2)$ 230 nM
$K_i(D_3)$ 4 nM	**$K_i(D_3)$ 7 nM**	$K_i(D_3)$ 170 nM
$K_i(D_4)$ 35 nM	**$K_i(D_4)$ 2.3 nM**	**$K_i(D_4)$ 21 nM**
$K_i(D_5)$ 130 nM	$K_i(D_5)$ 100 nM	$K_i(D_5)$ 330 nM

Figure 4. The first atypical antipsychotic clozapine in comparison with typical antipsychotics.

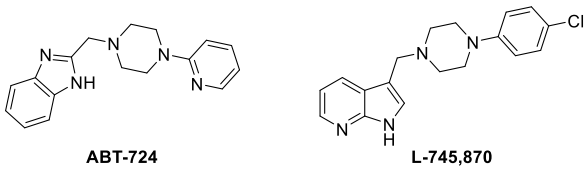

ABT-724

$K_i(D_2)$ >10000 nM
$K_i(D_4)$ 64 nM
D_2/D_4 = 156
*c*Log*P* 2.61

L-745,870

$K_i(D_2)$ 960 nM
$K_i(D_4)$ 0.43 nM
D_2/D_4 = 2233
*c*Log*P* 3.31

Figure 5. D_4 selective receptor ligands **ABT-724** and **L-745,870** with binding affinities and calculated Log*P* values (ChemDraw 16).

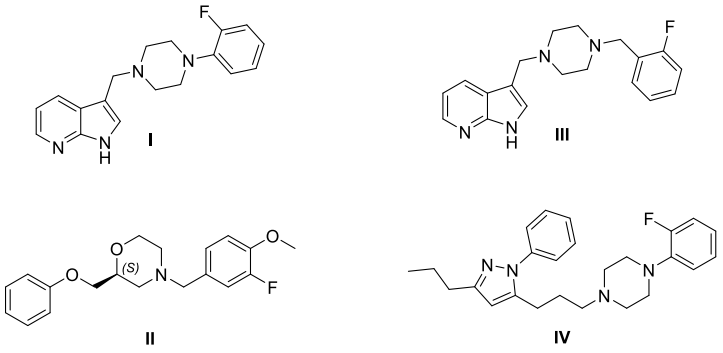

Figure 6. Compounds selected for binding studies.

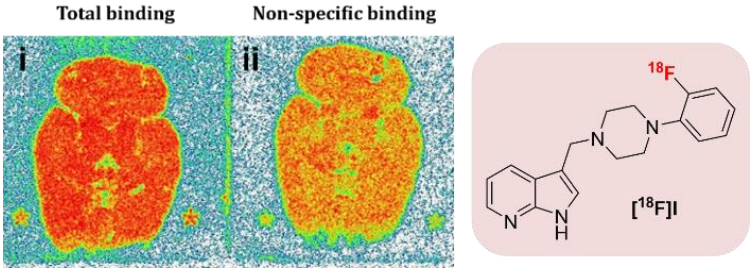

Figure 4. *In vitro* autoradiography of horizontal rat brain slices with 2.31 kBq/mL [^{18}F]**I** alone (Total binding) or after blocking with 5 µM non-labeled **I** (Non-specific binding). i) Total binding profile. ii) Competition with non-radioactive [^{19}F]**I**, displaying non-specific binding.

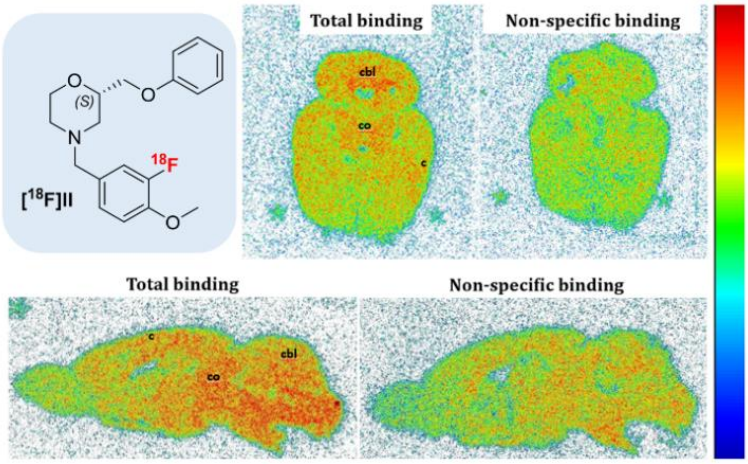

Figure 5. *In vitro* autoradiography of horizontal (top) and sagittal (bottom) rat brain slices with 2.31 kBq/mL **[^{18}F]II** alone (Total binding) or after blocking with 5 µM non-labeled **II** (Nonspecific binding). cbl: cerebellum, co: colliculi, c: cortex).

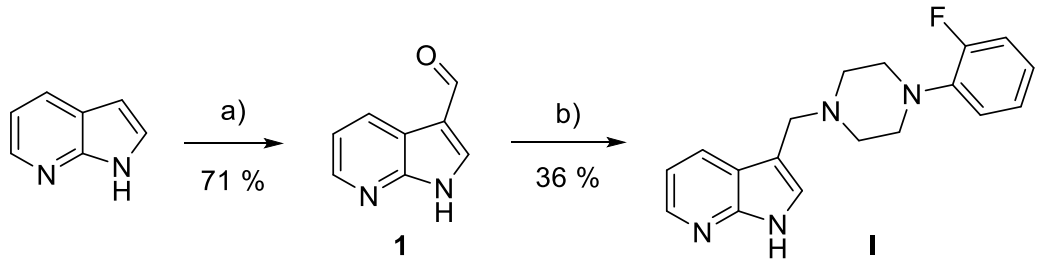

Scheme 3. Synthesis of reference compound **I** a) Hexamethylenetetramine (HMTA, 120 °C, 6 h). b) 1-(2-fluorophenyl)piperazine, $NaBH_3CN$, pH 5 (AcOH), 80 °C, 15 h.

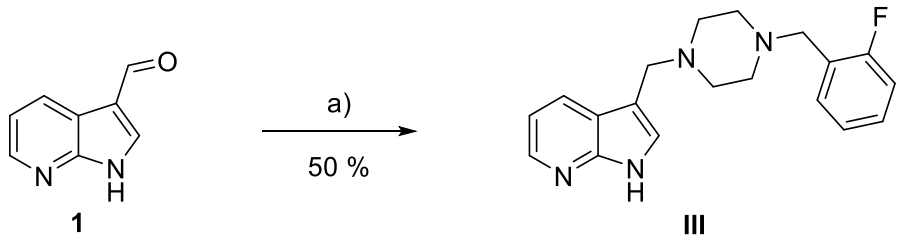

1 III

Scheme 4. Synthesis of reference compound **III** a) 1-(2-fluorobenzyl)piperazine, $NaBH_3CN$, pH 5 (AcOH), 80 °C, 15 h.

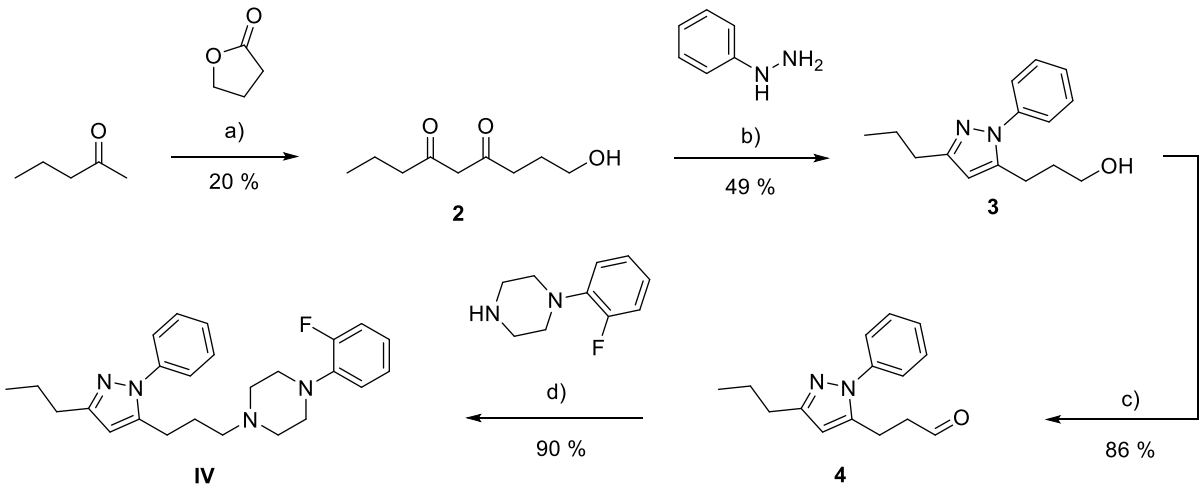

Scheme 3. Synthesis of reference compound **IV** a) NaOMe, benzene, 30-50 °C. b) TEA 3 eq., MeOH, r.t., 4 h. c) DMP, DCM, r.t., 12 h. d) $NaBH_3CN$, MeOH, 80 °C, 12 h.

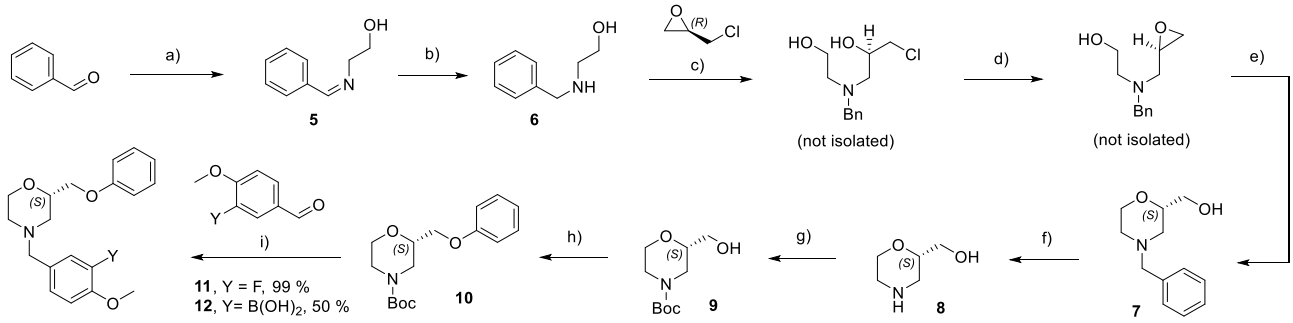

Scheme 4. Synthesis of labeling precursor **22** and reference compound **II** a) 2-aminoethanol, toluene b) $NaBH_3CN$, r.t., 12 h. c) (*R*)-epichlorhydrine d&e) 20 wt-% aq. Et_4NOH, 2-PrOH/H2O (1:1) f) 10 % Pd-C, NH_4CO_2H, MeOH g) guanidine*HCl, di-*tert*-butyl dicarbonate, EtOH h) phenol, PPh_3, diisopropyl azodicarboxylate (DIAD), THF, 40 kHz, 15 min i) HCl, $NaBH_3CN$, MeOH, 60 °C, 12 h.

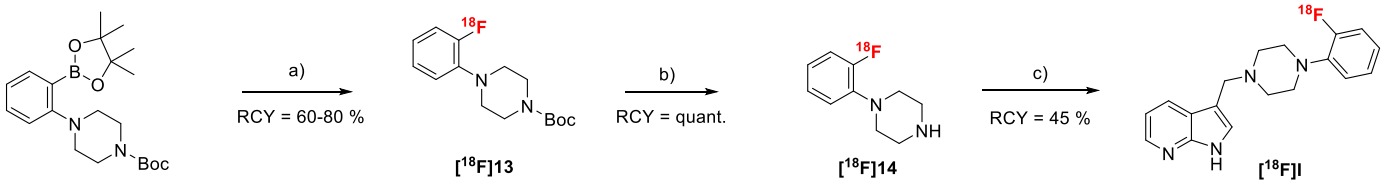

Scheme 5. Synthesis of compound [^{18}F]**I** a) Elution of ^{18}F- with Et_4NHCO_3 in *n*BuOH; $[Cu(OTf)_2(py)_4]$, DMA, 110 °C, 10 min. b) TFA, 110 °C, 20 min. c) **3**, $NaBH_3CN$, 80 °C, 5 min. (RCY determined by radio-HPLC).

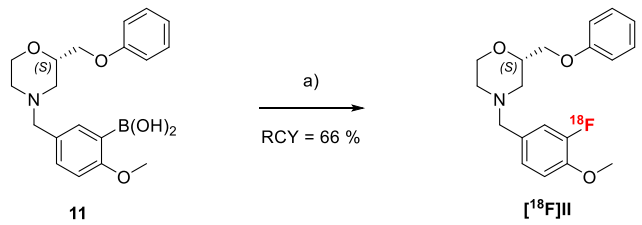

Scheme 6. Synthesis of compound **[^{18}F]II** a) Elution of $^{18}F^-$ with Et_4NHCO_3 in *n*BuOH; $[Cu(OTf)_2(py)_4]$, DMA, 110 °C, 10 min.

Tables:

Table 1. Receptor binding affinities of fluorine-substituted candidate ligands **I-IV** to the human dopamine receptor subtypes, serotonin and adrenergic receptors.

	K_i ± SD [nM][a]			
	I	II	III	IV
hD_1R [b]	7300 ± 1100	4800 ± 1300	18000 ± 2800	290 ± 7.1
hD_5R [b]	51000 ± 4900	8100 ± 1800	71000 ± 20000	1000 ± 0
hD_2Rlong [c]	1400 ± 710	470 ± 110	14000 ± 710	40 ± 4.2
$hD_2Rshort$ [c]	960 ± 480	450 ± 120	14000 ± 2100	27 ± 6.4
hD_3R [c]	2400 ± 920	3600 ± 920	36000 ± 9900	59 ± 9.2
$hD_{4.4}R$ [c]	4.1 ± 1.5	13 ± 4.2	18 ± 7.1	6.4 ± 0.6
$h5\text{-}HT_{1A}R$ [d]	14000 ± 5700	7900 ± 210	17000 ± 0	180 ± 14
$h5\text{-}HT_{2A}R$ [e]	560 ± 210	7400 ± 1800	6000 ± 710	22 ± 14
$h\alpha_{1A}$ [f]	69 ± 12	280 ± 0	2000 ± 1100	1.2 ± 0.1

[a] Ki values are the mean of two independent experiments ± SD each done in triplicates;

[b] [^{3}H]SCH 23990; [c] [^{3}H]spiperone; [d] [^{3}H]WAY600135; [e] [^{3}H]ketanserin; [f] [^{3}H]prazosin

Table 2. D_4 receptor subtype selectivity of fluorine-substituted ligands **I-IV**.

	$K_i(hD_{4.4}R)$	Ratio K_i / $K_i(hD_{4.4}R)$							
	[nM]	hD_1R	hD_5R	hD_2R_{long}	hD_2R_{short}	hD_3R	$h5\text{-}HT_{1A}R$	$h5\text{-}HT_{2A}R$	$h\alpha_{1A}$
I	4.1 ± 1.5	1800	12000	340	230	590	3400	140	17
II	13 ± 4.2	370	620	36	35	280	610	570	22
III	18 ± 7.1	1000	3900	780	780	2000	940	330	110
IV	6.4 ± 0.6	45	160	6.3	4.2	9.2	28	3.4	0.2

Table 3. Calculated logP and $logD_{7.4}$ values for the fluorine-substituted ligands **I-IV**.

	I	**II**	**III**	**IV**
***c*logP**				
ALOGPS 2.1	2.84	2.94	2.09	5.57
ChemDraw 16	2.91	3.25	2.57	6.19
Chemicalize	3.04	3.38	2.88	5.66
***c*logD$_{7.4}$**				
Chemicalize	2.71	3.38	2.51	5.12